Computer simulation of bistable switching in a nematic device containing pear-shaped particles

BARMES, F. and CLEAVER, D. J.

Published version

BARMES, F. and CLEAVER, D. J. (2006). Computer simulation of bistable switching in a nematic device containing pear-shaped particles. Chemical physics letters, 425 (1-3), 44-48.

Computer simulation of bistable switching in a nematic device containing pear-shaped particles.

F. Barmes [a,*] and D.J. Cleaver [b]

[a] *Centre Européen de Calcul Atomique et Moléculaire, 46, allée d'Italie, 69007 Lyon, France.*

[b] *Materials and Engineering Research Institute, Sheffield Hallam University, Sheffield S1 1WB, United Kingdom.*

Abstract

We study the microscopic basis of bistable switching of a confined liquid crystal via Monte Carlo simulations of hard pear-shaped particles. Using both dielectric and dipolar field couplings to this intrinsically flexoelectric fluid, it is shown that pulsed fields of opposing polarity can be used to switch between the vertical and hybrid aligned states. Further, it is shown that the field-susceptibility of the surface polarisation, rather than the bulk flexoelectricity, is the main driver of this switching behaviour.

Flexoelectricity is an effect by which an applied bulk field can induce polar director field gradients in a mesophase such as a nematic liquid crystal (LC) [1]. Essentially, it provides a mechanism by which to impose splay and bend distortions of a given polarity on a mesophase which is otherwise centrosymmetric. Microscopically, this phase polarisation arises due to a combination of the action of the field on molecular dipoles and some steric or electrostatic asymmetry in the molecule-molecule interactions [2–4]. Interest in flexoelectricity, particularly its microscopic origins, has been reignited recently due to the development of liquid crystal displays (LCD's) which exploit bistable surface anchoring of the nematic phase [5,6]. Several switching mechanisms have been proposed for these devices such as the use of competing dielectric and flexoelectric couplings to the applied field [7], the inclusion of electrochiral ions [8] or self-assembled hydrogen-bonded fibers [9] or, finally, the use of field-induced surface defects [10] whose density can even be used to achieve a grey-scale device.

* Corresponding author :
F. Barmes (frederic.barmes@cecam.org)

Following the lead of Barberi and co-workers [7,10], Davidson and Mottram recently showed that a flexoelectric nematic subject to directional field pulses can execute two-way switching in an LC cell with one monostable homeotropic substrate and one bistable planar/homeotropic substrate [11]. Specifically, by considering both dielectric and flexoelectric couplings to homogeneous applied fields, within an Ericksen-Leslie theory approximation, they identified a narrow parameter window for two-way switching between vertical (V) and hybrid aligned nematic (HAN) states.

However, the model used in this study was somewhat simplified when one considers the full range of polar contributions present in real systems: the flexoelectric polarisation can itself be resolved into director-gradient and order parameter gradient terms (the latter being termed the 'order electric' polarisation); ion migration effects are known to be significant for the LC mixtures and substrate materials used in prototype devices [12]; and molecular polarisation (or ferroelectric order) in the substrate region is known to be present in many confined LC systems [13,14]. The simplification associated with Davidson and Mottram's approach is echoed in the recent debate on how best to partition between these different polar terms when using HAN cells to measure flexoelectric coefficients. For HAN cells subject to applied fields, measured director profile distortions are poorly described by director flexoelectricity alone [15]; strong cases have been made to compensate for this with either surface polarisation [16] or ion-distribution terms [17], whereas Lattice-Boltzmann simulations indicate significant near-surface order electricity [18]. In practice, then, there is evidence to suggest that a combination of all three of these effects commonly operates in concert with director flexoelectricity.

Here, we consider the microscopic basis of directional-pulsed-field switching in such systems using Monte Carlo simulations of hard pear-shaped particles confined in slab geometry. This particle shape is used since, following the original arguments of Meyer [2], its mesophases exhibit splay flexoelectricity. The interparticle interactions are implemented using the parametric hard gaussian overlap (PHGO) approach introduced in [19]; we use the parameterisation with elongation $k = 5$ shown, in Ref. [19], to possess both nematic and smectic A_2 phases, the latter being a bilayer smectic phase with layers formed perpendicular to the director. Being based on a purely steric single-site interaction, this is a particularly efficient model for use here, though similar behaviour can be expected for any of the generic flexoelectric particle models introduced in recent years [20–22]. Investigation of two-way HAN-V switching also requires a bistable particle-substrate interaction potential and a particle-field coupling which induces competition between the dielectric and flexoelectric terms. The latter is achieved here by taking each pear to interact with an applied field through both dielectric and dipolar terms. Thus

$$U_i^{\text{field}} = -\frac{1}{2}\Delta\chi\left(\mathbf{E}\cdot\hat{\mathbf{u}}_i\right)^2 - \mu\left(\mathbf{E}\cdot\hat{\mathbf{u}}_i\right) \tag{1}$$

where $\Delta\chi$ is the anisotropy in the dielectric susceptibility, μ is the dipole moment, $\hat{\mathbf{u}}_i$ the particle orientation and $\mathbf{E} = E\hat{\mathbf{z}}$ the applied electric field. Note that electrostatic particle-particle interactions are neglected in this study on the basis that, as in Ref. [20], they play a minor role. Similarly, in all simulated systems, we follow Davidson and Mottram in adopting the common approximation that $\mathbf{E}$ is constant rather than imposing a fixed voltage drop and calculating $\mathbf{E}(\mathbf{z})$ based on instantaneous dielectric profiles and an assumption of constant electric displacement.

Following the approach taken in our previous studies of liquid crystal anchoring [23,24], the pear-shaped particles do not interact directly with the constraining substrates. Instead, particle-substrate interactions are mediated through objects embedded within the mesogenic particles (see Fig. 1). The benefit of this approach is that changing the shapes of such embedded objects provides a microscopic mechanism by which to control the orientation (i.e. homeotropic, tilted or planar) and nature (monostable or bistable; strong or weak) of the resultant anchoring. Here we use centrosymmetric (i.e. ellipsoid-like) HGO particles for the embedded objects, so as to take advantage of the strong homeotropic-planar bistability region previously determined for the HGO-planar substrate surface potential [24]. To prevent the HGO particles from protruding outside their host particles, the former are shifted along the particle axes (towards the bulky end of each pear) so as to make the endpoints of the embedded and host particles coincide (see Fig. 1). This results in a polar particle-substrate interaction, since the points of the pears are left free to penetrate the substrate plane; the extent of this allowed penetration and, hence, the relative stability of the homeotropic anchoring state are controlled by k_S, the length-to-breadth ratio of the embedded object. The particle-substrate interactions are, then, given by

$$\mathcal{V}_i^{\text{Pear-Surface}} = \begin{cases} 0 \ \text{ if } |z_{\text{obj},i} - z_0| \geq \sigma_w^{\text{HGO-Surface}} \\ \infty \ \text{ if } |z_{\text{obj},i} - z_0| < \sigma_w^{\text{HGO-Surface}} \end{cases} \tag{2}$$

where z_0 defines the substrate plane and $z_{\text{obj},i}$ is the z-coordinate of the object embedded in pear i:

$$z_{\text{obj},i} = z_i - \frac{\sigma_0}{2}\,(k - k_S)\cos\theta_i. \tag{3}$$

Here z_i and θ_i are, respectively, the z-coordinate and zenithal angle of pear i and σ_0 sets the particle width. $\sigma_w^{\text{HGO-Surface}} = \sigma_0 \left[(1 - \chi_S \sin^2\theta)/(1 - \chi_S)\right]^{1/2}$ is the HGO-surface contact distance [24] and $\chi_S = (k_S^2 - 1)/(k_S^2 + 1)$ is the shape anisotropy of the embedded HGO particles. The ratio k_S/k is restricted to the range $[0.4 : 0.8]$.

Before HAN-V switching was investigated, the surface anchoring properties of

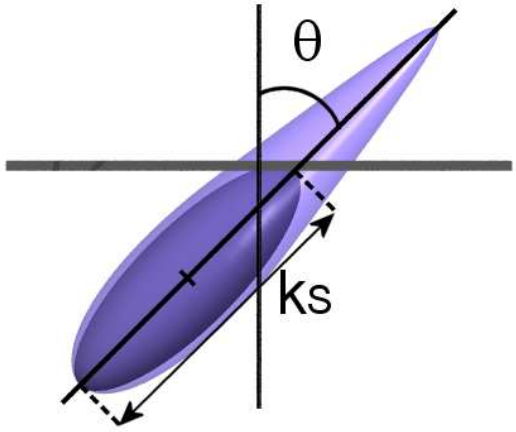

Fig. 1. Schematic representation of the interaction between a pear shaped particle of elongation k and a planar substrate (shown as a horizontal bar). The interaction is mediated by an ellipsoidal HGO particle of elongation k_S embedded in the pear and shifted along the molecular axis to make the ends of the two objects coincident.

the potential Eqn.(2) were characterised by means of preliminary simulations using systems of $N = 1000$ particles confined symmetrically between identical substrates. A slab geometry of height $L_z = 4k\sigma_0$ along $\hat{\mathbf{z}}$ was used, periodic boundary conditions being applied in the $\hat{\mathbf{x}}$ and $\hat{\mathbf{y}}$ directions. The surfaces located at $z = L_z$ and $z = -L_z$ will be subsequently referred to as the top and bottom surfaces respectively.
The simulations were performed at constant nematic number density $\rho^* = 0.15$ and in series of increasing and decreasing k_S. From these runs, a homeotropic to planar anchoring transition was identified from the behaviour of $\overline{Q_{zz}^{Su}}(\rho^*, k_S/k)$ (see [23] for a definition), the density-profile-weighted average of the order tensor element $Q_{zz}(z)$ in the interfacial regions. These data, shown in Fig. 2, indicate a discontinuous transition between the homeotropic and planar states, corresponding, respectively, to positive and negative $\overline{Q_{zz}^{Su}}(\rho^*, k_S/k)$, for $0.64 \leq k_S/k \leq 0.74$. The hysteresis identified from series of simulations performed with, respectively, increasing and decreasing k_S/k suggests a region of bistability which is maximal for $k_S/k = 0.7$. Though not apparent from the data shown in Fig. 2, the homeotropic state observed here exhibits considerable surface polarisation since the interaction potential (2) only allows the points of the pears to penetrate the substrate plane.

When attempting to transfer this behaviour to a hybrid anchored system, it was found that imposing strong, monostable homeotropic anchoring (i.e. small k_S) at the top (*i.e.* maximum z-value) surface resulted in the loss of bistability at the bottom (*i.e.* minimum z-value) surface. This situation is known to prevail in very thin films when one anchoring coefficient is significantly larger than the other [25,26] since the dominant surface extrapolation length is then able to exceed the film thickness. To recover bistability at the bottom surface, therefore, the slab thickness was increased and the top surface anchoring

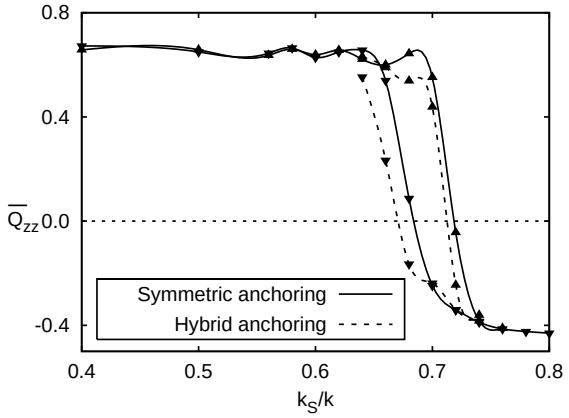

Fig. 2. Behaviour of $\overline{Q_{zz}^{Su}}$ as a function of the reduced embedded object elongation k_S/k for pear shaped PHGO particles in symmetric and hybrid confining geometries. In the case of hybrid anchoring, only the particles near the bistable substrate are considered. ▲ indicate simulation runs with increasing k_S/k while ▼ indicate simulation runs performed with decreasing k_S/k.

strength reduced (by increasing the k_S value used). As shown in Fig. 2, an acceptable degree of bistability was obtained for a double-thickness slab (i.e. $L_z = 8k\sigma_0$, $N = 2000$) with $k_S/k = 0.6$ and ~ 0.7 at the top and bottom surfaces, respectively. The use here of different values for k_S/k at the top and bottom surfaces simply results in the particles interacting with each substrate in a different way, just as if each substrate had a different surface treatment.

The two-way switching identified by Davidson and Mottram requires an appropriate balance of the dielectric and dipolar coupling terms. The dipolar term needs to be sufficiently strong to latch the lower region of the cell into a configuration that will equilibrate into the vertical state on removal of the field. However, the E^2 coupling of the dielectric term dictates that *it* dominates (re-establishing the HAN state) at high field values. In initial assessment of HAN to V switching, runs performed with $k_BT = 1.0$, $\Delta\chi = -1.0$ and $\mu = 1.0$, and a range of E values, fields more negative than $E = -0.4$ led to domination by the dielectric term. However, a field $E = -0.2$ was found to induce significant but unsaturated deviation of the director profile away from its initial state. None of these systems relaxed to the V state on removal of the field, so further runs were performed with $E = -0.2$ and gradually increased dipolar coupling strengths μ in the range [1.0-3.5]. For each of these cases, the slab was subjected to consecutive extended runs of 2.5×10^5 sweeps (where one sweep is one attempted move per particle) with the field applied and, then, removed. The $Q_{zz}(z)$ profiles obtained indicate that the $\mu = 2.0$ system exhibited substantial director distortion throughout the bulk region of the cell but no switching. For $\mu = 2.5$, by contrast (Fig. 3(a)), the director distortion was concentrated in the lower half of the slab, a configuration which, on removal of the field, successfully switched into the vertical state. Configuration snapshots showing the HAN to V switching behaviour of this $\mu = 2.5$ system are given

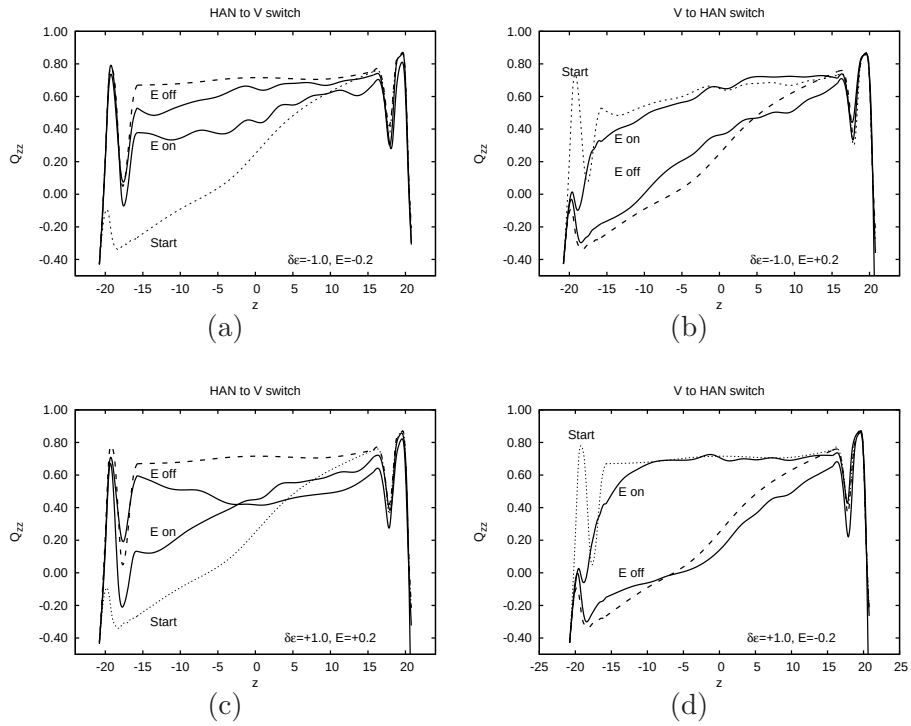

Fig. 3. $Q_{zz}(z)$ profiles corresponding to each stage of the two way switching between the HAN to V states using $\mu = 2.5$ and $\mathbf{E} = \pm 0.2\hat{\mathbf{z}}$. Subfigures (a) and (b) show the results obtained using $\Delta\chi = -1.0$ while subfigures (c) and (d) show those for $\Delta\chi = +1.0$. The dotted lines show the starting configurations and the dashed lines typical target HAN and V profiles.

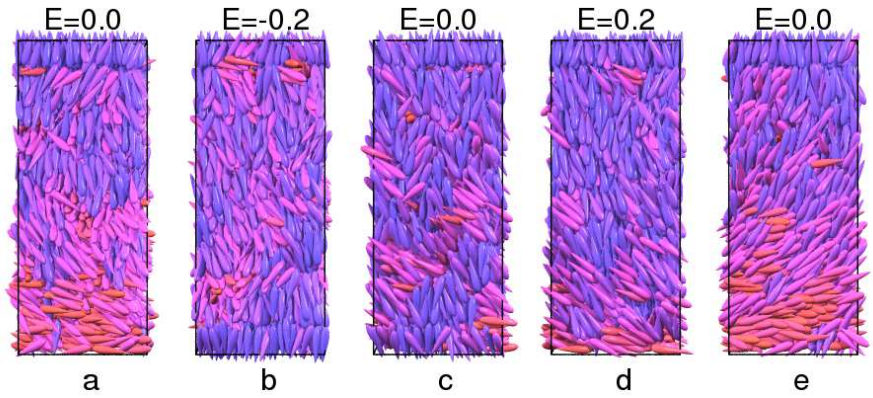

Fig. 4. Configuration snapshots illustrating reversible switching of a system with $\mathbf{E} = \pm 0.2\hat{\mathbf{z}}$, $\Delta\chi = -1.0$ and $\mu = 2.5$.

in Figs. 4(a)-(c).

Taking the final configuration from this sequence and then performing a similar sequence with an equal but opposite applied field led to the $Q_{zz}(z)$ profiles shown in Fig. 3(b). Here, upon application of the field, most of the vertically-aligned slab remained undistorted but a narrow region near the bottom surface

developed features compatible with planar anchoring. Upon removal of the field, this small region proved sufficient to seed its planar orientation into the bulk part of the cell, leading to recovery of the HAN state. Configuration snapshots illustrating this reverse (V to HAN) switching are given in Figs. 4(c)-(e). Note that this reverse switching process became less accessible for higher dipole couplings due to the consequent reduction in the thickness of the planar surface region. In practice, no reverse switching was observed for $\mu > 3.5$.

While our simulations have successfully reproduced the reversible pulse-field-induced switching predicted by Davidson and Mottram [11], the $Q_{zz}(z)$ profiles shown in Fig. 3 are significantly different from those obtained using the director-flexoelectricity-based approach. Specifically, the "E on" profile of Fig. 3(b) is homeotropically aligned for positive z and has a bend from homeotropic-to-planar for negative z. In comparison, the corresponding profiles (marked with positive E values) in Davidson and Mottram's Fig. 5 are largely planar for low z but bent in the high z region. To assess this further, we have repeated our simulation procedure for the alternative parameterization $\Delta\chi = 1.0$, $\mu = 2.5$ and $E = \pm 0.2$, *i.e.* the same numerical values but with the opposite sign for the dielectric anisotropy ; see Fig. 3(c-d). Here, we have again observed reversible switching between the HAN and V states. However, the $Q_{zz}(z)$ profiles obtained from these positive $\Delta\chi$ switching runs are qualitatively identical to those given in Figs. 3(a-b), whereas Davidson and Mottram's calculations predict a marked dependence on the sign of the dielectric coupling term. These qualitative differences raise the possibility that competition between bulk dielectric and flexoelectric couplings is *not* the main driver for the reversible switching observed in our simulations.

In seeking to examine this suggestion, we note that the bulk flexoelectric coupling considered by Davidson and Mottram is, in their constant E approximation of Ericksen-Leslie theory, equivalent to a *centrosymmetric* effective surface term proportional to $\cos(2\theta)$[11]. Closer examination of our simulation results, conversely, indicates that the field dependence of the *surface polarisation* plays the dominant role. Thus, for $\mathbf{E} = -0.2\hat{\mathbf{z}}$ (Figs. 3(a) and 4(b)) the top surface polarisation (and, consequently, anchoring strength) is reduced by the applied field while that at the lower surface shows an even stronger field-susceptibility: the negative applied field leads to a highly polar homeotropic surface layer, with the pear points embedded in the substrate. Equivalently, the positive applied field destabilises this polar homeotropic state at the lower substrate, promoting, instead, planar surface alignment (Figs. 3(b) and 4(d)). As noted above, the effective surface term associated with bulk-region flexoelectricity has no polar component and so cannot have driven all of this behaviour. We conclude, therefore, that the switching observed in this system was induced by the direct action of the applied field to produce a *polar* surface-region anchoring field.

Clear temperature susceptibility of the surface polarisation has been observed experimentally for 5CB at both planar and homeotropic substrates [14]. While no field-dependence was noted for the surface polarisations inferred from isothermal measurements on HAN cells [15], differences between the monostable substrates used in these cells and the weakly-anchored bistable substrate employed in our simulations is not unexpected. The dominance of surface polarisation over bulk flexoelectric effects in our simulated systems is likely related to the thinness of the film employed; the influence of flexoelectric distortions is effectively integrated across a LC film and, so, is inevitably reduced for the film thicknesses accessible to molecular simulation (the slab thickness employed here corresponds to approximately 50nm). Notwithstanding this proviso, our results demonstrate that surface polarisation and, in particular, its field susceptibility, can play a significant role in HAN-V switching through its influence on surface anchoring strength and stability. Consequently, such polarisation changes appear able to affect the orientational structure of the confined films, as well as providing a mechanism for generating voltage offsets.

References

[1] P.G. de Gennes, The Physics of Liquid Crystals, 2nd ed., Clarendon press, 1993.

[2] R.B. Meyer, Piezoelectric effects in liquid crystals, Phys. Rev. Letts. 22 (1969) 918.

[3] J. Prost and J.P. Marcerou, On the microscopic interpretation of flexoelectricity, J. de Phys. 38 (1977) 315.

[4] J.P. Mearcerou and J. Prost, The different aspects of flexoelectricity in nematics, Mol. Cryst. Liq. Cryst. 58 (1980) 259.

[5] G.P. Bryan-Brown, C.V. Brown, I.C. Sage and V.C. Hui, Voltage-dependent anchoring of a nematic liquid crystal on a grating surface, Nature 392 (1998) 365.

[6] S. Kitson, A. Geisow, Controllable alignment of nematic liquid crystals around microscopic posts: Stabilization of multiple states, App. Phys. Letts. 80 (19) (2002) 3635–3637.

[7] R. Barberi, M. Giocondo, D. Durand, Flexoelectrically controlled surface bistable switching in nematic liquid crystals, App. Phys. Letts. 60 (1992) 1085.

[8] R. Barberi, D. Durand, Electrochirally controlled bistable surface switching in nematic liquid crystals, App. Phys. Letts. 58 (1991) 2907.

[9] N. Mizoshita, Y. Suzuki, K. Hanabusa, T. Kato, Bistable nematic liquid crystals with self-assembled fibers, Adv. Mat. 17 (2005) 692.

[10] R. Barberi, M. Giocondo, J. Li, R. Bartolino, I. Dozov and G. Durand, Fast bistable nematic display with grey scale, App. Phys. Letts. 71 (1997) 3495.

[11] A.J Davidson and N.J. Mottram, Flexoelectric switching in a bistable nematic device, Phys. Rev. E 65 (2002) 051710.

[12] J. C. Jones, S. Beldon, P. Brett, M. Francis, M. Goulding, Low voltage zenithal bistable devices with wide operating windows, SID 03 (2003) 26.3.

[13] B. Jerome, Surface effects and anchoring in liquid-crystals, Rep. Prog. Phys. 54 (3) (1991) 391.

[14] L. M. Blinov, M. I. Barnik, H. Ohaka, N. M. Shtykov, K. Yoshino, Surface and flexoelectric polarization in a nematic liquid crystal 5CB, Eur. Phys. J. E 4 (2001) 183.

[15] A. Mazzulla, F. Ciuchi, J. R. Sambles, Optical determination of flexoelectric coefficients and surface polarization in a hybrid aligned nematic cell, Phys. Rev. E 64 (2) (2001) 021708.

[16] A. Mazzulla, F. Ciuchi, J. R. Sambles, Reply to "comment on 'optical determination of flexoelectric coefficients and surface polarization in a hybrid aligned nematic cell' ", Phys. Rev. E 68 (2) (2003) 023702.

[17] G. Barbero, L. R. Evangelista, Comment on "optical determination of flexoelectric coefficients and surface polarization in a hybrid aligned nematic cell", Phys. Rev. E 68 (2) (2003) 023701.

[18] T. J. Spencer, Lattice boltzmann method for q-tensor nemato-dynamics in liquid crystal display devices, Ph.D. thesis, Sheffield Hallam University (April 2005).

[19] F. Barmes, M. Ricci, C. Zannoni and D.J. Cleaver , Computer simulations of pear shaped particles, Phys. Rev. E 68 (2003) 021708.

[20] R. Berardi, M. Ricci, C. Zannoni, Ferroelectric and structured phases from polar tapered mesogens, Ferroelectrics 309 (2004) 3.

[21] J. L. Billeter, R. A. Pelcovits, Molecular shape and flexoelectricity, Liq. Cryst. 27 (9) (2000) 1151–1160.

[22] J. Stelzer, R. Berardi, C. Zannoni, Flexoelectric coefficients for model pear shaped molecules from monte carlo simulations, Mol. Cryst. Liq. Cryst. 352 (2000) 621–628.

[23] F. Barmes and D.J. Cleaver , Computer simulations of a liquid crystal anchoring transition, Phys. Rev. E 69 (2004) 061705.

[24] F. Barmes and D.J. Cleaver , Using particle shape to induce tilted and bistable liquid crystal anchoring, Phys. Rev. E 71 (2005) 021705.

[25] D. J. Cleaver, P. I. C. Teixeira, Discontinuous structural transition in a thin hybrid liquid crystal film, Chem. Phys. Lett. 338 (2001) 1.

[26] A. Šarlah, S. Žumer, Equilibrium structures and pretransitional fluctuations in a very thin hybrid nematic film, Phys. Rev. E 60 (1999) 1821.